

Analysis of Oligosaccharide Conformation by NMR Spectroscopy Utilizing ^1H , ^1H and ^1H , ^{13}C Residual Dipolar Couplings in a Dilute Liquid Crystalline Phase

Kristina Lycknert,[†] Arnold Maliniak,[‡] and Göran Widmalm^{*,†}

Department of Organic Chemistry and Division of Physical Chemistry, Arrhenius Laboratory, Stockholm University, S-106 91 Stockholm, Sweden

Received: January 24, 2001

A novel procedure for determining ^1H , ^1H NMR dipolar couplings in a dilute liquid crystalline medium based on ^1H , ^1H COSY spectroscopy and a J -doubling procedure is presented. Subsequent conformational analysis of the central region of a partially deuterated decasaccharide employing ^1H , ^1H and ^1H , ^{13}C dipolar couplings, ^1H , ^1H nuclear Overhauser effect spectroscopy, and computer modeling is described. In particular, the use of ^1H , ^1H dipolar couplings is of paramount importance in deriving a three-dimensional structure of the decasaccharide.

Introduction

Analysis of molecular conformation has for a considerable time relied on measurements of the nuclear Overhauser effect (NOE), through-bond electron-mediated spin–spin (J) couplings, or a combination of these techniques. Both stereochemical and conformational aspects have been addressed in this way. These methods suffer, however, from serious limitations: interpretation of J couplings requires a physical model that provides a relationship between the spin–spin coupling and the molecular structure, while the NOEs are strongly dependent on dynamical processes in the molecule. Another tool for molecular structure determination is provided by long-range through-space magnetic dipole–dipole interactions. Dipolar couplings (D) depend on spin–spin distances and on the orientations of the internuclear vectors with respect to the magnetic field. In isotropic liquids, the dipolar interactions are averaged to zero due to the rapid molecular tumbling. The distance dependence of these interactions may be recovered from the cross-relaxation rates, while angular dependence is lost.

In anisotropic systems, such as liquid crystals,¹ measurements of dipolar couplings provide an extremely powerful tool for structure determination. Recently, application of dilute liquid crystalline phases formed by molecular aggregates, known as bicelles (disk shaped micelles), has been introduced for studies of macromolecules.² The magnetic susceptibility of the aggregates results in an orientation within the magnetic field of the spectrometer. This orientation leads to an anisotropic environment experienced by nonspherical “solute” molecules, which results in an NMR spectrum with observable dipolar couplings. Heteronuclear ^1H , ^{15}N and ^1H , ^{13}C residual dipolar couplings have been measured for different types of biomolecules such as nucleic acids,³ proteins⁴ and carbohydrates.^{5–13} In an NMR spectrum, we observe the sum of spin–spin and dipolar interactions. Since the heteronuclear one-bond J couplings are rather large, the measurement of the dipolar contributions is relatively simple, enabling detection of both negative and positive values. In contrast, determination of homonuclear

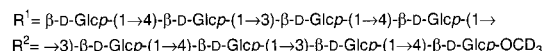
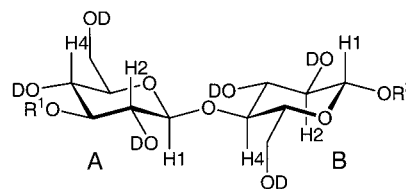


Figure 1. Schematic of the decasaccharide. The six protons present in the molecule are indicated. The two sugar residues of the central cellobiose fragment are denoted A and B, and protons on these residues are named accordingly. The glycosidic torsion angles ϕ and ψ are defined as H1A-C1A-O4B-C4B and C1A-O4B-C4B-H4B , respectively.

^1H , ^1H dipolar couplings presents a problem since the magnitude is similar to the spin–spin couplings. These couplings contain, however, important information about the molecular structure. In particular, the ^1H , ^1H couplings over the glycosidic linkage provide a powerful tool for the determination of the three-dimensional structure of carbohydrates. Recently, one route to determining the ^1H , ^1H dipolar couplings in a carbohydrate system,¹⁴ was described. It is based on the collection of different constant time COSY spectra and subsequent analysis of the observed ratio of cross-peak and autpeak amplitudes. In proteins, the sign of the homonuclear dipolar coupling can be determined in relation to a known ^1H , ^{15}N coupling.¹⁵ Here we present a novel approach to extract the ^1H , ^1H D couplings. These were combined with heteronuclear ^1H , ^{13}C dipolar couplings and classical ^1H , ^1H NOE spectroscopy in the analysis of the conformation of the central residues of a specifically deuterium labeled decasaccharide.

Results and Discussion

The decasaccharide¹⁶ consists of D-Glc residues with alternating β -(1 \rightarrow 3) and β -(1 \rightarrow 4) linkages (Figure 1). The two central residues denoted A and B correspond to a cellobiose building block. Only six protons are present in the molecule, namely, H1, H2, and H4, as indicated. The conformation at a glycosidic linkage is described by the two torsion angles ϕ and ψ . The distances between trans glycosidic protons are thus

* Corresponding author. E-mail: gw@organ.su.se.

[†] Department of Organic Chemistry.

[‡] Division of Physical Chemistry.

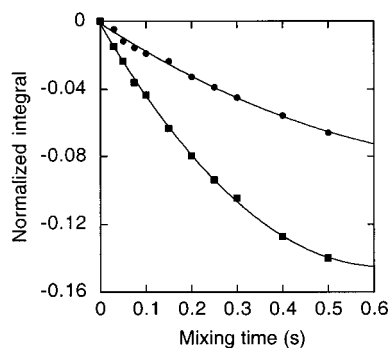


Figure 2. $^1\text{H}, ^1\text{H}$ NOE buildup curves for the intraresidue H4B-H2B spin-pair (b), which is used as the reference interaction in the ISPA distance calculations and the trans glycosidic H4B-H1A spin-pair (9).

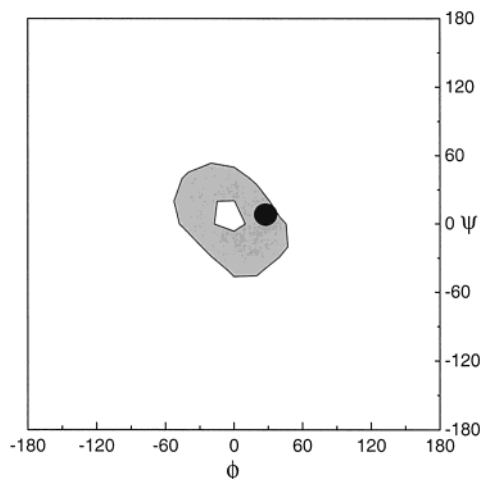


Figure 3. Ramachandran map generated in 10° increments using the CHARMM program (Molecular Simulations Inc., San Diego, CA) of the conformational space of the central glycosidic linkage in the deca-saccharide. The region consistent with $^1\text{H}, ^1\text{H}$ NOE data is shown in gray, and the conformation consistent with the dipolar coupling data is indicated by the black filled circle.

determined by a combination of these torsions. In the deca-saccharide, the protons H1A and H4B are anticipated to be close in space so that a $^1\text{H}, ^1\text{H}$ NOE may be observed. The resonance of the H4B proton was selectively inverted¹⁷ in a 1D DPFGE NOESY experiment¹⁸ and the cross-relaxation to H1A and H2B were monitored as NOE buildup curves (Figure 2). For the proton pairs, the isolated spin pair approximation (ISPA) was used to obtain the cross-relaxation rates (σ). The intraring distance, H4B-H2B, is assumed to be quite well defined by the $^4\text{C}_1$ conformation of the glucosyl residue. From molecular modeling, using three different force fields, the reference distance was estimated to be $2.6 \pm 0.1 \text{ \AA}$. The trans glycosidic distance, H4B-H1A, was 2.2 \AA as calculated from the relationship $r_{ij} = r_{\text{ref}}(\sigma_{\text{ref}}/\sigma_{ij})^{1/6}$. Using a ψ grid search, a conformational region consistent with the trans glycosidic distance of $2.2 \pm 0.1 \text{ \AA}$ can be identified and is shown in Figure 3. The experimentally accessible distance restraints across a glycosidic linkage are usually scarce. Therefore, additional experimental observables are necessary to obtain a more complete picture of the conformation at a certain glycosidic linkage.

The heteronuclear $^1\text{H}, ^{13}\text{C}$ residual dipolar couplings in the two sugar residues were calculated by subtraction of the $^1J_{\text{C,H}}$ values in the isotropic phase from the apparent F_1 splitting in a coupled $^1\text{H}, ^{13}\text{C}$ HSQC spectrum¹⁹ obtained in the ordered phase.²⁰ The three C-H vectors within each sugar residue orient in a parallel fashion with D couplings of 22 Hz in residue A

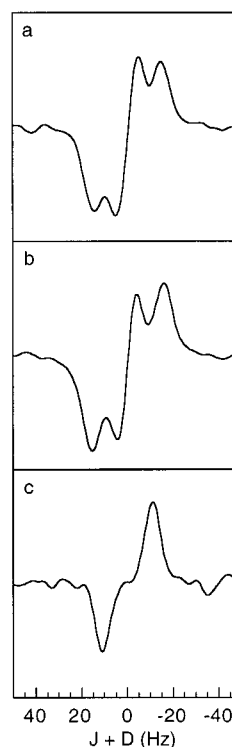


Figure 4. F_2 slices of the cross-peaks in the phase-sensitive $^1\text{H}, ^1\text{H}$ DQF-COSY spectrum of the deca-saccharide in the ordered phase showing homonuclear $J + D$ couplings. (a) H4B to H1A slice at δ for H4B (antiphase splitting only D coupling); (b) H1A to H4B slice at δ for H1A; (c) H2B to H4B slice at δ for H2B (antiphase splitting $J + D$ coupling with significant cancellation).

and 20 Hz in residue B (note though that the J values differed by some 20 Hz between different positions within the sugar residues). The experimental error of the heteronuclear D couplings is estimated to be 2 Hz. Thus, the C-H vectors in the two central residues of the deca-saccharide exhibit similar orientation in the molecular frame.

We now turn to the measurement of the homonuclear $^1\text{H}, ^1\text{H}$ dipolar couplings. These were extracted from a $^1\text{H}, ^1\text{H}$ DQF-COSY spectrum²¹ recorded in the ordered phase. In analogy with the heteronuclear case the observed splittings are sums of $J + D$. We employ, however, a slightly different method for the analysis of the spectra. This method is known as J -doubling²² in the frequency domain²³ and was previously used to extract $^3J_{\text{C,H}}$ values across glycosidic linkages.²⁴ The technique is particularly useful for estimating coupling constants in crowded multiplets.²⁵ Here we apply the J -doubling procedure for measurements of the combined contribution from the spin-spin and dipolar couplings. Identifying that the $^1\text{H}, ^1\text{H}$ COSY spectrum has an antiphase splitting for an active coupling (and an in-phase splitting for a passive one), we set out to try to measure the $^1\text{H}, ^1\text{H}$ dipolar couplings in the ordered phase. The J values extracted in the isotropic phase using the J -doubling procedure were in good agreement with their counterparts obtained from direct measurement in a one-dimensional ^1H NMR spectrum in the isotropic phase. It was not possible to obtain the homonuclear D couplings from a one-dimensional ^1H NMR spectrum, inter alia, because of the nondeuterated chemicals used to produce the ordered phase. Selected F_2 slices are shown in Figure 4. Excellent agreement of D was obtained for each pair of F_2 -sliced cross-peaks at different sides of the diagonal, i.e., different chemical shifts. The dipolar coupling is largest for H1A-H4B (Figure 4a and 4b) across the glycosidic linkage, where also the J coupling is negligible. The small

TABLE 1: ^1H , ^1H Couplings for the Decasaccharide

atom pair	$ J + D $ (Hz)	D (Hz) ^a
H1A–H2A	12	4
H1B–H2B	11	3
H2B–H4B	11	–11
H1A–H4B	19	–19

^a Sign inferred from analysis (see text).

difference seen in the peak appearance is due to the different values of the passive couplings in the cross-peaks. The peak for H2B–H4B (Figure 4c) reveals substantial cancellation of the doublets leaving only the outer peaks. Thus, in Figure 4, increasing cancellation occurs from panels a to c. When J is very small, it is not possible to determine the sign of D using the above-described procedure. The experimental dipolar couplings are summarized in Table 1. However, the H2A–H4A D coupling was not obtainable due to complete chemical shift overlap.¹⁶ Employing the J -doubling procedure, it has been shown that J couplings can be determined very accurately.²⁶ In the present analysis, we estimate the experimental error of the homonuclear D couplings to be below 1 Hz.

The expression for the dipole–dipole couplings in a uniaxial liquid crystal is given by

$$D_{ij} = -\frac{\mu_0}{4\pi} \frac{\gamma_i \gamma_j}{2\pi r_{ij}^3} \left[\frac{1}{2} (3 \cos^2 \theta_0 - 1) \left[S_{zz} \frac{1}{2} (3 \cos^2 \theta_{ij}^z - 1) + (S_{xx} - S_{yy}) \frac{1}{2} (\cos^2 \theta_{ij}^x - \cos^2 \theta_{ij}^y) \right] \right] \quad (1)$$

where r_{ij} is the spin–spin distance, θ_{ij}^α ($\alpha = x, y, z$) are angles between the spin–spin vector and the molecular coordinate frame, and the order parameters, $S_{\alpha\alpha}$, are the elements of the ordering matrix.¹ The angle θ_0 (here $\theta_0 = 90^\circ$) defines the relative orientation of the magnetic field and the director. All other symbols have their usual meaning. Note that two important assumptions have been introduced in eq 1: A single ordering matrix is used, indicating a rigid molecule. The presence of internal motion requires additional order parameters. In principle, the expression for every dipolar coupling should be scaled by an appropriate order parameter, S , that reflects the flexibility of the spin–spin vector. The second, and more important, approximation concerns the choice of the molecular coordinate frame. In the most general case (no symmetry operations on the molecule or molecular fragment), the ordering tensor contains five order parameters (S_{zz} , $S_{xx} - S_{yy}$, S_{xy} , S_{xz} , and S_{yz}), and consequently, at least five dipolar couplings are required for a complete description of the orientational order. However, if the location of the principal axes for the ordering matrix is known, only two diagonal elements, S_{zz} and $S_{xx} - S_{yy}$, are necessary. In the present case, we have access to five independent dipolar couplings, which is sufficient to determine the ordering frame for the molecule, but no structural information can then be inferred. We choose therefore another, much simpler, approach and assume that the ordering coordinate frame corresponds to the principal axis system of the moment of inertia tensor. On the basis of computer simulations, we have previously evaluated the effect of different definitions of the molecular frames in a nematic liquid crystal²⁷ and found the moment of inertia tensor to be a reasonable approximation for a flexible molecule.

In our analysis, eq 1 was numerically fitted to the experimental sets of homo- and heteronuclear dipolar couplings. To determine the molecular coordinate frame, we have performed a metropolis Monte Carlo computer simulation²⁸ on the entire

TABLE 2: Analysis of the Dipolar Couplings

structure number	torsion	angle ($^\circ$) ψ	H1A–H4B (\AA)	$-S_{zz}$ (10^{-3})	$S_{xx} - S_{yy}$ (10^{-3})	fitting error
1	30	10	2.17	4.2	0.14	0.070
2	10	30	2.21	3.8	0.38	0.076
3	40	0	2.20	4.4	0.04	0.077
4	20	20	2.19	3.8	0.32	0.088
5	40	–10	2.18	4.8	0.16	0.095

decasaccharide (in vacuo) using the hard sphere *exo*-anomeric approach.²⁹ The simulation predicted average torsion angles $= 53^\circ$ and $\psi = 10^\circ$ for the β -(1f 4) linkages, whereas the corresponding values for the β -(1f 3) linkages were 51° and -3° . We have used these torsion angles for all residues in the molecule, except for the central cellobiose fragment in the analysis presented below.

The fitting procedure comprised 18 structures of this fragment with different values of the torsion angles and ψ . All structures were consistent with the NOE restriction at the glycosidic linkage, i.e., a distance of 2.2 \AA between H1A and H4B (Figure 3), and were generated using a grid search procedure. An additional complication that needs to be mentioned is the sign of the two couplings H2B–H4B and H1A–H4B. Since the spin–spin contribution for these is essentially zero, we are not able to determine the absolute sign of the dipolar interaction. Thus, in the analysis, we need to consider four possible situations: two with equal signs and two with opposite signs. The orientations of the dipolar vectors in the molecular coordinate frame, i.e., the angles θ_{ij}^α were determined by calculating the moment of inertia tensor for every structure. Two free parameters were used in the analysis: S_{zz} and $S_{xx} - S_{yy}$. The quality of the analysis is determined by the fitting error

$$\text{error} = N^{-1} \sum_{i < j} |D_{ij}^{\text{exp}} - D_{ij}^{\text{calc}}| / |D_{ij}^{\text{exp}}| \quad (2)$$

Initially, we noted that the experimental dataset assuming opposite signs of the dipolar couplings H2B–H4B and H1A–H4B produced very large fitting errors. These cases were therefore rejected in further considerations. In the subsequent analysis, we found that the fitting errors were much smaller when the two couplings were assumed to be negative. This result is also consistent with the picture where the molecule is oriented with the axis defined by C4A and C1B atoms parallel to the magnetic field. In fact, this vector deviates by only $\sim 15^\circ$ from the principal component of the moment of inertia tensor. Such a molecular orientation requires negative H2B–H4B and H1A–H4B couplings. The results for selected structures are shown in Table 2. Note, that the molecular biaxiality is very small ($S_{zz} \gg S_{xx} - S_{yy}$), which gives support to our approximation about the molecular frame. It should be stressed, however, that even a small biaxiality of the ordering tensor can be of crucial importance in the analysis of the dipolar couplings.³⁰ The small fitting errors indicate an extremely good correlation; in fact, for the best structure, the deviation did not exceed 2 Hz for any coupling. In addition, we calculated the H2A–H4A D coupling (not measured, vide supra) using the parameters derived from the analysis and found it to be -3.2 Hz.

Finally, we note, that the choice of the molecular frame is important because it reflects the ordering of the entire decasaccharide in the liquid crystal. Analysis performed on the cellobiose fragment only; i.e., neglecting R¹ and R² tetrasaccharide fragments (Figure 1) produced a best fit structure with the torsion angles $= -30^\circ$ and $\psi = 20^\circ$. This is a conformational region not anticipated to be highly populated,

in particular with respect to the negative value of the torsion angle.³¹ Instead, the present solution with $\approx 30^\circ$ and $\psi \approx 10^\circ$ is in fact quite similar to that obtained from the Monte Carlo simulation per se and consistent with the *exo*-anomeric effect²⁹ governing the conformation at β , which should be positive for the β -D-Glcp residues present in the decasaccharide.

We have shown that the utilization of different NMR techniques, in particular, ^1H , ^1H dipolar couplings, in combination with molecular modeling is a powerful tool in determining structural aspects of biomolecules such as oligosaccharides.

Materials and Methods

The synthesis of the decasaccharide has been described previously.¹⁶ Cetylpyridinium chloride (CPCI) and sodium chloride (NaCl) were purchased from Merck (Darmstadt, Germany), and *n*-hexanol was obtained from BDH Chemicals (Poole, England), all with a purity >98%. The chemicals were used without further purification.

The CPCI/*n*-hexanol/brine (200 mM NaCl in D_2O) sample was prepared by weight to give concentrations of 3.5% (w/v) with respect to the total content of CPCI/*n*-hexanol, where the two components were added in equal amount. To the brine/surfactant solution, *n*-hexanol was added, and the sample was vortexed. This was followed by equilibration first at 70 °C and then at 30 °C for at least 1 h each.

The homogeneity of the dilute liquid crystals was checked in the NMR spectrometer by the ^2H quadrupolar splitting in D_2O . Sharp lines of equal height are obtained when the sample is homogeneous. At this point, the decasaccharide was dissolved in the liquid crystalline solvent to give a sugar concentration of 0.8 mM. Spectra of the CPCI/*n*-hexanol/brine preparation (ordered phase) and a 200 mM brine solution (isotropic phase) were acquired at 30 °C. The resulting ^2H quadrupolar splitting was 9.6 Hz.

NMR experiments were performed on a Varian Inova 600 MHz spectrometer using a 5 mm PFG triple resonance probe. Proton–proton cross-relaxation rates in the decasaccharide were measured in the brine solution using the one-dimensional DPGSE NOESY experiment. Selective excitation at the resonance frequency of H4B was enabled using an i-Snob-2 shaped pulse¹⁷ of 68 ms duration. Spectra were recorded using a spectral width of 2100 Hz and 8192 complex points, sampling 320 transients at each mixing time. Ten different cross-relaxation delays (mixing times) between 30 and 500 ms were used. Prior to Fourier transformation, the FIDs were zero-filled four times and multiplied with a 1 Hz exponential line-broadening factor. Spectra were baseline corrected using a first-order correction and integrated using the same integration limits at all mixing times. ^1H , ^1H cross-relaxation build-up curves were obtained from the normalized integrals at different mixing times, and the rates were calculated by fitting to a second-order polynomial.

The carbon–proton splittings were measured employing the ^1H , ^{13}C -gHSQC technique. The experiment was performed with spectral widths of 1.7 kHz for ^1H and 10.6 kHz for ^{13}C using a modified pulse sequence where the peak separation was measured in the indirect dimension. In both phases, 128 transients of 1024 complex points were accumulated for 512 increments. The spectra were zero-filled four times in t_1 and once in t_2 prior to the spectral analysis.

Phase-sensitive ^1H , ^1H DQF-COSY spectra were measured with 128×2048 complex points in t_1 and t_2 , respectively, using a spectral width of 3.9 kHz. Prior to Fourier transformation (FT), zero-filling to 1024×4096 complex points was performed. *J*, *D*, and *J* + *D* couplings were extracted from F_2 slices (inverse

FT, zero-filling eight times, FT) as antiphase splittings using the *J*-doubling procedure with eight delta functions in the frequency domain.

A metropolis Monte Carlo (MC) simulation was carried out using the GEGOP program (version 2.7) with a force field based on the hard sphere *exo*-anomeric approach, which makes use of rigid carbohydrate residues. The simple potential includes only the τ -torsion and van der Waals interactions. A total of 2×10^6 MC steps were performed with an acceptance ratio of 24%. The glycosidic torsion angles were not allowed to move more than 8° in an MC step.

Acknowledgment. This work was supported by grants from the Swedish Research Council and the Carl Trygger Foundation.

References and Notes

- (1) Emsley, J. W., Ed. In *Nuclear Magnetic Resonance of Liquid Crystals*; Reidel: Dordrecht, The Netherlands, 1985.
- (2) Tjandra, N.; Bax, A. *Science* **1997**, *278*, 1111–1114.
- (3) Hansen, M. R.; Mueller, L.; Pardi, A. *Nat. Struct. Biol.* **1998**, *5*, 1065–1074.
- (4) Sass, J.; Cordier, F.; Hoffmann, A.; Rogowski, M.; Cousin, A.; Omichinski, J. G.; Löwen, H.; Grzesiek, S. *J. Am. Chem. Soc.* **1999**, *121*, 2047–2055.
- (5) Ram, P.; Mazzola, L.; Prestegard, J. H. *J. Am. Chem. Soc.* **1989**, *111*, 3176–3182.
- (6) Rundlöf, T.; Landersjö, C.; Lycknert, K.; Maliniak, A.; Widmalm, G. *Magn. Reson. Chem.* **1998**, *36*, 773–776.
- (7) Bolon, P. J.; Prestegard, J. H. *J. Am. Chem. Soc.* **1998**, *120*, 9366–9367.
- (8) Kiddle, G. R.; Homans, S. W. *FEBS Lett.* **1998**, *436*, 128–130.
- (9) Martin-Pastor, M.; Bush, C. A. *Carbohydr. Res.* **2000**, *323*, 147–155.
- (10) Martin-Pastor, M.; Bush, C. A. *Biochemistry* **2000**, *39*, 4674–4683.
- (11) Landersjö, C.; Höög, C.; Maliniak, A.; Widmalm, G. *J. Phys. Chem. B* **2000**, *104*, 5618–5624.
- (12) Tian, F.; Al-Hashimi, H. M.; Caighead, J. L.; Prestegard, J. H. *J. Am. Chem. Soc.* **2001**, *123*, 485–492.
- (13) Staaf, M.; Höög, C.; Stevansson, B.; Maliniak, A.; Widmalm, G. *Biochemistry* **2001**, *40*, 3623–3628.
- (14) Tian, F.; Bolon, P. J.; Prestegard, J. H. *J. Am. Chem. Soc.* **1999**, *121*, 7712–7713.
- (15) Peti, W.; Griesinger, C. *J. Am. Chem. Soc.* **2000**, *122*, 3975–3976.
- (16) Hällgren, C.; Widmalm, G. *J. Carbohydr. Chem.* **1993**, *12*, 309–333.
- (17) Kupce, E.; Boyd, J.; Campbell, I. D. *J. Magn. Reson., Ser. B* **1995**, *106*, 300–303.
- (18) Stott, K.; Keeler, J.; Van, Q. N.; Shaka, A. J. *J. Magn. Reson.* **1997**, *125*, 302–324.
- (19) Willker, W.; Leibfritz, D.; Kerssebaum, R.; Bermel, W. *Magn. Reson. Chem.* **1993**, *33*, 287–292.
- (20) Porte, G.; Gomati, R.; El Haitamy, O.; Appell, J.; Marignan, J. *J. Phys. Chem.* **1986**, *90*, 5746–5751.
- (21) Piantini, U.; Sørensen, O. W.; Ernst, R. R. *J. Am. Chem. Soc.* **1982**, *104*, 6800–6801.
- (22) McIntyre, L.; Freeman, R. *J. Magn. Reson.* **1992**, *96*, 425–431.
- (23) del Río-Portilla, F.; Blechta, V.; Freeman, R. *J. Magn. Reson., Ser. A* **1994**, *111*, 132–135.
- (24) Rundlöf, T.; Kjellberg, A.; Damberg, C.; Nishida, T.; Widmalm, G. *Magn. Reson. Chem.* **1998**, *36*, 839–847.
- (25) Jones, J. A.; Grainger, D. S.; Hore, P. J.; Daniell, G. J. *J. Magn. Reson., Ser. A* **1993**, *101*, 162–169.
- (26) Garca-García, A.; Ponzanelli-Velázquez, G.; del Río-Portilla, F. *J. Magn. Reson.* **2001**, *148*, 214–219.
- (27) Komolkin, A. V.; Laaksonen, A.; Maliniak, A. *J. Chem. Phys.* **1994**, *101*, 4103–4116.
- (28) Stuike-Prill, R.; Meyer, B. *Eur. J. Biochem.* **1990**, *194*, 903–919.
- (29) Thøgersen, H.; Lemieux, R. U.; Bock, K.; Meyer, B. *Can. J. Chem.* **1982**, *60*, 44–57.
- (30) Tjandra, N.; Tate, S.-i.; Ono, A.; Kainosho, M.; Bax, A. *J. Am. Chem. Soc.* **2000**, *122*, 6190–6200.
- (31) Asensio, J. L.; Cañada, F. J.; Cheng, X.; Khan, N.; Mootoo, D. R.; Jiménez-Barbero, J. *Chem. Eur. J.* **2000**, *6*, 1035–1041.